Article citation info:
KORTA J, SKRUCH P. The concept of integrating vapor chamber into a housing of electronic devices for increased thermal reliability. Eksploatacja i Niezawodnosc – Maintenance and Reliability 2020; 22 (2): 363–369, http://dx.doi.org/10.17531/ein.2020.2.19.

Jakub KORTA
Paweł SKRUCH

THE CONCEPT OF INTEGRATING VAPOR CHAMBER INTO A HOUSING OF ELECTRONIC DEVICES FOR INCREASED THERMAL RELIABILITY

KONCEPCJA INTEGRACJI KOMORY PAROWEJ Z OBUDOWĄ UKŁADÓW ELEKTRONICZNYCH W CELU ZWIĘKSZENIA ICH NIEZAWODNOŚCI*

Systematic increase in computational power and continuous miniaturization of automotive electronic controllers pose a challenge to maintaining allowable temperature of semiconductor components, preventing premature wear-out or, in extreme cases, unacceptable shutdown of these devices. For these reasons, efficient and durable cooling systems are gaining importance in modern car technology design, showing critical influence on reliability of vehicle electronics. Vapor chambers (flat heat pipes) which could support heat management of automotive electronic controllers in the nearest future are passive devices, which transport heat through evaporation-condensation process of a working liquid. At present, vapor chambers are not commercially used in cooling systems of automotive controllers, being a subject of research and development endeavors aimed at understanding their influence on thermomechanical reliability of semiconductor devices used in cars. This paper presents a concept of an electronic controller aluminum housing integrated with a vapor chamber. The conceptual design was numerically validated in elevated temperature, typical for automotive ambient conditions. The paper discusses influence of the vapor chamber-based cooling system on the controller's thermal performance, as well as on its reliability, expressed as the expected lifetime of the device.

Keywords: *cooling, electronics, thermal analysis, heat pipe, vapor chamber, phase change, automotive, reliability.*

Systematycznie wzrastająca moc obliczeniowa oraz postępująca miniaturyzacja urządzeń elektronicznych stosowanych w pojazdach samochodowych powodują trudności w utrzymaniu temperatury pracy elementów półprzewodnikowych w dozwolonym zakresie, przyczyniając się do ich przedwczesnego zużycia, a w skrajnych przypadkach, uniemożliwiając nawet ich normalną pracę. Wydajne i trwałe układy chłodzące stają się więc nieodzownym komponentem współczesnych podzespołów samochodowych, o krytycznym znaczeniu dla ich niezawodności. Urządzeniami mogącymi w niedalekiej przyszłości wspomagać działanie układów chłodzenia systemów elektronicznych wykorzystywanych w motoryzacji są komory parowe (płaskie rurki cieplne), w których transport energii termicznej zachodzi poprzez przemianę fazową i samoistne przemieszczanie się czynnika roboczego. Współcześnie, tego rodzaju urządzenia nie są komercyjnie stosowane w układach chłodzenia sterowników samochodowych, pozostając przedmiotem prac badawczo-rozwojowych związanych z ich wpływem na szeroko pojętą niezawodność termomechaniczną urządzeń elektronicznych. W niniejszym artykule opisano koncepcję zintegrowania komory parowej z aluminiową obudową kontrolera elektronicznego pracującego w warunkach podwyższonej temperatury otoczenia, odpowiadającej warunkom użytkowania komponentów samochodowych. Ponadto, ocenie poddano wpływ zastosowania tego urządzenia na temperaturę pracy chłodzonego elementu półprzewodnikowego i jego niezawodność, wyrażoną jako przewidywany czas jego bezawaryjnego funkcjonowania.

Słowa kluczowe: *chłodzenie, elektronika, analiza termiczna, rurka cieplna, komora parowa, przemiana fazowa, motoryzacja, niezawodność.*

1. The need for cooling of electronic devices

In the recent years, high-power electronic devices have been gaining more and more interest in the automotive industry. This type of devices is used to increase vehicle comfort and safety performances. High-end automotive electronics is also utilized in multimedia equipment (infotainment) and various types of driver assistance systems, collectively called as ADAS (Advanced Driver Assistance Systems). Operation principle of ADAS devices is based on acquisition of various types of signals – generated by wireless communication systems, cameras, radars, ultrasonic transducers or lidars – and its high-performance processing. For safety reasons, the latter is frequently performed in near real time.

Acquisition and analysis of such big data streams requires utilization of significant computing powers, which results in an undesirable side effect of generation of large amounts of thermal energy. In consequence, this often leads to considerable rise in operating temperature of electronic components, resulting in premature wear-out or, in extreme cases, causing sudden shutdown of these components during operation, which is unacceptable for human safety reasons. Another important factor is the ambient temperature to which the ADAS systems are exposed. Automotive-grade components must typically operate in 50°C or more, which makes it difficult to maintain semiconductor chips within allowable operating temperature limits. Following the results presented in [20], high operating temperature was the reason for 49% of recalls in the automotive market, in the 2005-2015 period. As described in [6,16], alongside mechanical vibration, long-term high temperature exposure and temperature cycling are the main factors of electronics failure.

It is forecasted, that despite continuous development and optimization of computing algorithms and improvements of hardware tech-

(*) Tekst artykułu w polskiej wersji językowej dostępny w elektronicznym wydaniu kwartalnika na stronie ***www.ein.org.pl***

nology, the value of heat fluxes generated by complete automotive electronic systems (in particular automated driving controllers) will rise to 1kW and above [8]. In order to make operation of these systems possible, new cooling solutions for vehicle electronics are being developed, which must meet the automotive requirements, that is, be thermally efficient, characterized by high degree of reliability and be low-cost, allowing for large scale production. Such cooling systems must allow for dissipation of high density heat fluxes, being a result of generating several dozen of watts on a surface of a single semiconductor device die (typically, several square centimeters). An example of such a device is Nvidia Xavier system-on-a-chip, dedicated to autonomous driving tasks, for which the TDP (thermal design power) is 30W, generated on a die surface area equal to 3.5cm^2.

The undesired influence of elevated temperature on electronic devices is broadly described in the scientific and engineering literature. The authors of [10] described an overview of temperature-driven failure mechanisms of semiconductor devices and the influence of these phenomena on device reliability. Temperature cycling effect on reliability of high-power automotive transistors is described in [18]. In [11], the authors discussed an attempt to assess fatigue resistance of a car electronic controller components, loaded by variable operating temperature. A novel methodology of conducting accelerated temperature aging tests is proposed in [19]. The authors of [22] presented a methodology of predicting electronic devices reliability, which is based on the so-called PoF (physics of failure) model, incorporating the influence of die temperature on thermomechanical behavior of semiconductor device. Analysis of temperature effect on expected lifetime duration of contemporary ADAS electronic devices and systems is described in [4]. The same paper provides an insight into a methodology allowing for diagnosis of this sort of problems in the early stage design phase. A detailed description of up-to-date analytical and experimental methods for assessment of electronic devices reliability is presented in [5]. Two-phase cooling solutions, based on liquid evaporation – condensation cycle, and its application to electronics heat management is described in [1] and [3]. Both of these papers describe active cooling systems which were used to dissipate thermal energy to the ambient. Despite high cooling capacity, this type of solutions are rarely used in the automotive sector, due to the need for costly and space-occupying auxiliary devices, that is, heat exchangers, pumps, valves, hoses and others. The authors of [13] described phase change phenomenon and its exploitation in a passive cooling device – VC (vapor chamber), building and validation of numerical model describing VC behavior and its comparison to the efficiency of copper heat spreader. Similar study is presented in [17], which provides thorough characterization of vapor chambers and copper heat spreaders, used to disperse heat from semiconductor devices. In both, [13] and [17], the two-phase devices have been identified as superior over standard copper plates.

Despite great popularity of two-phase cooling devices in consumer electronics, there is a limited number of reports available in the public domain, describing its application in the automotive industry. The author of [12] provides a general overview of possible implementations of VC and heat pipes in road vehicles. The following regions of possible applications are enlisted in this work: temperature control of LED headlamps, electric vehicle battery pack cooling systems and heat management of electronic control units. An attempt of using heat pipes to dissipate thermal energy from a motorcycle headlamp equipped with LEDs is described in [15]. By comparison to the classical solution, the proposed two-phase cooling provided small improvement to the estimated lifetime duration of the headlamp. Application of VC to dissipate heat from a high power transistor module is studied in [14]. According to the findings presented in this paper, the use of VC resulted in decreased operating temperature of the transistors by ca. 9°C compared to a standard, copper-based solution. Simultaneously, application of VC decreased the temperature gradient measured on the analyzed device, positively influencing mechanical reliability of the module. Automotive radio passive cooling system based on a heat pipe is described in [9]. The device was tested in room conditions, in natural convection cooling. With respect to the solution based on an aluminum radiator, the two-phase cooling system provided ca. 3°C reduction in temperature of the main heat source component.

This paper describes a concept of integrating a small VC into an aluminum housing of an electronic device operating in ambient temperature typical for automotive environment. The aim of the presented analysis was to understand the influence of using flat heat pipe on the junction temperature (t_j) of the main heat source device and to estimate the change in the expected failure-free operating lifetime of this component. Considering limited number of studies available in the public domain and dedicated to passive, two-phase cooling systems of vehicle controllers, this paper can be a valuable source of information for scientists and engineers working in the field of thermomechanical reliability of automotive-grade electronic devices.

Section 2 of the paper presents general classification of cooling methods used to control temperature of electronic devices and discusses physical mechanisms of heat transfer. Section 3 describes operating principles of two-phase cooling devices. The concept of VC integration with an aluminum housing of an electronic device is descried in Section 4. Section 5 discusses the effect of this modification to the expected operation lifetime duration of the device. Section 6 summarizes and concludes the paper.

2. Cooling methods of electronics

Cooling systems of electronics can be divided into two categories: passive and active systems. Cooling solutions belonging to the first group take advantage of natural mechanisms of heat exchange, that is, conduction, convection and radiation. Active cooling systems utilize auxiliary, externally powered devices, like fans or pumps, in order to enhance natural heat transfer processes.

Other concept of cooling technologies classification assumes a straightforward criterion of occurrence of phase change process: electronics cooling can be obtained by heat transfer with no phase change effect (e.g., natural or forced air convection) or by employing phase change cycles (e.g., the already mentioned evaporation – condensation process, which takes place in VCs). Selection of the appropriate cooling technique is driven by the values of heat flux and heat flux density, which must be removed from a device. In the automotive applications, passive cooling is preferred, because of maintenance-free character of this technology. Moreover, by contrast to the active solutions, passive cooling does not require external power supply, which improves the overall energy balance of the system.

Heat transfer mechanisms, that is, conduction, convection and radiation can be described by equations (1) – (3) [2]. In the case of heat conduction along a specified direction, the heat flow rate can be expressed by the equation (1):

$$\dot{Q} = -k\frac{\Delta TA}{\Delta x} \tag{1}$$

where: $\dot{Q}[\mathrm{W}]$ – heat flow ratio, $\Delta T[\mathrm{K}]$ – temperature difference measured along the heat flow, $\Delta x[\mathrm{m}]$ – flow distance, $A\left[\mathrm{m}^2\right]$ – cross-section area of the conductor, $k\left[\frac{\mathrm{W}}{\mathrm{m}\cdot\mathrm{K}}\right]$ – heat conductivity of the conductor material.

Heat convection is a macroscopic-scale phenomenon of heat transport, which takes place in fluids. Natural convection is driven by non-uniform fluid density, while forced convection is caused by external means, for example, operation of a fan or pump. Convective heat flow ratio can be described by equation (2):

$$\dot{Q} = Ah(T_s - T_\infty) \quad (2)$$

where: $T_s[\mathrm{K}]$ and $T_\infty[\mathrm{K}]$ – temperature measured on a heat source and at a distance, respectively, $h\left[\frac{\mathrm{W}}{\mathrm{m^2K}}\right]$ denotes convection heat transfer coefficient, which depends on shape, size, convection type and other factors.

Radiative heat transfer is driven by propagation of electromagnetic waves which are generated by movement of electrically charged particles. Similarly to convection and conduction, thermal radiation takes place in ambient temperatures above absolute zero. Heat radiated by a source in unit of time can be expressed by equation (3):

$$\dot{Q} = \varepsilon\sigma A\left(T_S^4 - T_A^4\right) \quad (3)$$

where: ε – dimensionless coefficient of thermal emissivity, $\sigma = 5.67x10^{-8}\left[\frac{\mathrm{W}}{\mathrm{K^4m^2}}\right]$ –Stefan – Boltzmann constant, $T_A[\mathrm{K}]$ – ambient temperature.

In reality, all three phenomena simultaneously participate in heat dissipation process, but it is a cooling system designer responsibility to decide on individual contribution of each heat transfer mechanism.

3. Phase change heat transfer

Efficient passive cooling systems are based on phase change heat transfer mechanism. In such solutions, the phase change is most frequently observed between liquid and gaseous phases, in the evaporation – condensation process. In cooling solutions of electronics, the phase change process is most commonly used in heat pipes and VCs. As schematically shown in Fig. 1, functionally separate regions can be distinguished in the body of these devices.

In the evaporator region, which is heated by an external heat source, working fluid changes its phase to vapor. The amount of thermal energy consumed in this process is equal to the liquid's latent heat of evaporation. The accumulated thermal energy is stored in the vapor and transported through the device cavity by natural convection process, towards the condenser region. Lower temperature of the condenser initializes heat transfer out of the vapor, causing reversed phase change process, that is, condensation. Simultaneously, pressure field inside the device causes condensed liquid to flow towards evaporator region. Liquid transport is enhanced by capillary forces between working medium and grooves or porous structures frequently embedded inside the device.

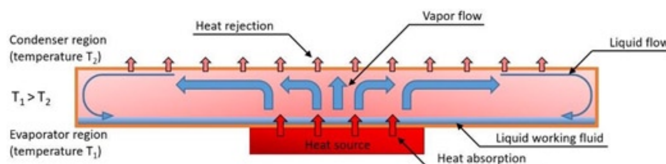

Fig. 1. Vapor chamber operating principle

In VCs integrated in consumer electronic devices, the most frequently used working medium is demineralized water. Other liquids, like methanol or acetone, are less popular due to higher level of toxicity and lower latent heat of evaporation h_e values they are characterized by. Table 1 combines h_e values for the mentioned working fluids.

The overall effect of using VC is continuous absorption of heat in the evaporator region, and its release in condenser area. Hence, thermal energy is continuously transported from source to opposite side of the device, where it can be easily dissipated to the ambient. Additionally, typically large VC condenser regions lead to a decrease in density of dissipated heat flux.

Table 1. Latent heat of evaporation for selected working fluids typically used in two-phase cooling [2].

Working fluid	Latent heat of evaporation $h_e\left[\frac{\mathrm{kJ}}{\mathrm{kg}}\right]$
Water	2257
Methanol	1100
Acetone	518

Subsequent paragraphs of this paper describe a concept of integrating a VC into aluminum housing of an electronic device. Thermal efficiency of this passive cooling system is compared with a standard solution, based on heat conduction in solid material of the enclosure. Assessment of both designs was done by means of numerical modelling and analysis by the CFD (Computational Fluid Dynamics) method.

4. Concept of vapor chamber integration into an electronics housing

Figure 2 depicts the two-part enclosure of the electronic device which was the subject of the described analyses. The housing was made from aluminum alloy EN AC-44300 ($k_{Al} = 130\frac{\mathrm{W}}{\mathrm{m\cdot K}}$) and covered by a number of fins, allowing for improved heat exchange with the surroundings. Additionally, Fig. 2 shows the header used to supply power and communicate with electronic devices inside the controller.

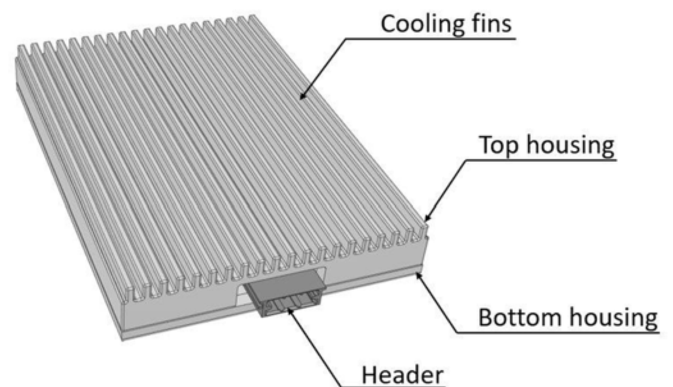

Fig. 2. The analyzed electronic device enclosed in an aluminum housing

The general view of the electronic device layout (i.e., PCB with electronic components) used in thermal analysis is shown in Fig. 3. Additionally, the analyzed model contained screws used for closing the assembly. One of the components (Component I) mounted on the PCB dissipated $P = 18\,\mathrm{W}$ of power, while the total power dissipation of the complete device reached 20.84W (Fig. 4). In the standard cooling solution which was analyzed in the first design iteration, Component I was connected to the aluminum housing through a pedestal. Additionally, a layer of thermal interface material was used between the heat source and aluminum pedestal, to decrease thermal interface resistance between these components. The model was simulated in elevated ambient temperature conditions, for which $t_{amb} = 55°\mathrm{C}$. The highest allowable junction temperature for Component I device was given by the chip manufacturer and was equal to $t_j^{max} = 125°\mathrm{C}$. Estimation of this value can be done by using equation (4), which requires

knowledge of maximum temperature on the top surface of the device t_{top}. The junction temperature, t_j can be then computed as [2]:

$$t_j = t_{top} + \left(\mathrm{R}_{\theta jc} \cdot P\right) \tag{4}$$

where $\mathrm{R}_{\theta jc}$ denotes thermal resistance coefficient between device top surface and junction. The value of this parameter was provided in the chip datasheet and, in the discussed case, was equal to $\mathrm{R}_{\theta jc} = 1.22 \frac{^{\mathrm{o}}\mathrm{C}}{\mathrm{W}}$.

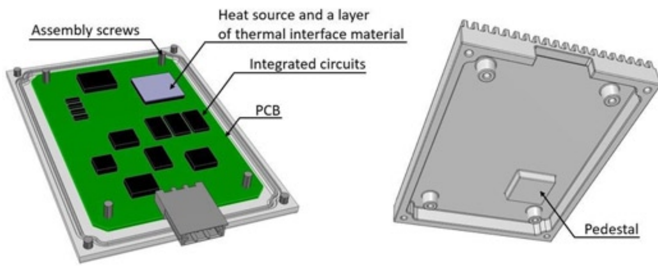

Fig. 3. *Inner view of the analyzed electronic device and housing equipped with a pedestal.*

4.1. Simulation results

The simulations described in this paper were carried out by means of CFD method, which allows for investigations of three-dimensional models and study the behavior of flow and heat transfer parameters in appropriate calculation space. In order to describe and solve the problem of finding the fluid flow pattern (in the discussed example the air was modelled inside and outside of the controller housing), the utilized CFD method numerically solves Navier – Stokes equations. Transport of thermal energy was considered in the calculation models by means of all three heat transfer mechanisms, that is, conduction, convection and radiation. It was assumed, that flow around the controller housing is laminar and that convective heat exchange is driven by natural convection, modelled by Boussinesq approximation. Heat radiation process was modelled by the well-known DO (Discrete Ordinates) approach, in which the radiation equation is solved along discrete number of directions established for every heat source. For accuracy, each radiation octant was divided into five angular steps, both in azimuthal and polar directions. Each simulated case was considered as a steady state problem. The numerical models prepared for the analysis consisted of ca. 4 millions of elements. Each simulation was stopped after residual values for the momentum, velocity and energy equations reached values below 10^{-4}, 10^{-4} i 10^{-8}, respectively. Additionally, temperature change observed on the top surface of the Component I heat source was negligible in every two consecutive solver iterations.

Figure 5 depicts the temperature field calculated on the surface of the PCB, Component I and other electronic devices, obtained for the standard cooling solution (pedestal above the main heat source). The temperature on the top surface of Component I reached in this case ca. 103.7°C.

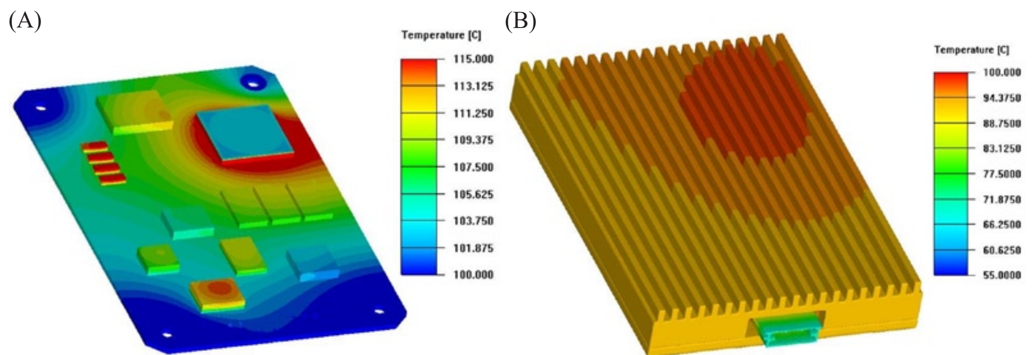

Fig. 5. *Results obtained for the device equipped with a standard cooling solution. Temperature field plotted for: PCB and electronic components (A) and top side of the housing (B)*

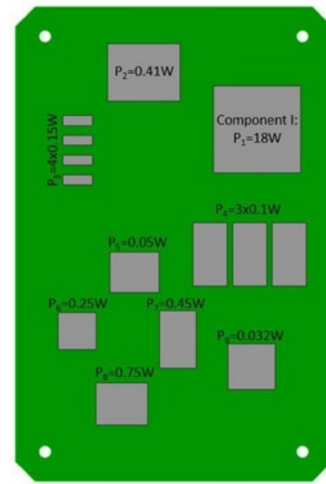

Fig. 4. *Power dissipated by the components of the analyzed electronic device.*

Junction temperature of this component was calculated using equation (4): $t_j = 103.7 + (1.22 \cdot 18) = 125.66$ °C. It exceeded slightly the allowable t_j^{max} limit of 125°C. However, possible variation with respect to the simulated operating conditions (e.g., accumulation of dirt on the housing surface and between the fins or strong thermal radiation from other devices), can cause further increase of t_j temperature. This, in turn, can lead to failure of the device and severely limit its operational lifetime.

In order to decrease the operating temperature of the controller components, in the subsequent design iteration, a VC was integrated into the housing of the device. This design modification was aimed at intensification of heat dissipation from the main heat source (Component I) to the fins on the top of the housing. It was assumed that demineralized water was the working fluid inside the VC. Additionally, the VC walls were made from copper, which is characterized by high heat conductivity value of $k_{Cu} = 385 \frac{\mathrm{W}}{\mathrm{m} \cdot \mathrm{K}}$. The external dimensions of this component were equal to 75x90x4mm. As shown in Fig. 6, the VC was positioned inside the housing to stay in contact simultaneously with top surface of the analyzed heat source and inner wall of the aluminum enclosure. To minimize the interface thermal resistance, in both of these joints a 0.5mm layer of thermal interface material was used. Thermal conductivity for the latter material was equal to $k = 3.5 \frac{\mathrm{W}}{\mathrm{m} - \mathrm{K}}$.

In order to effectively use the VC heat dissipation capability, inner top wall of the housing was modified by elimination of the pedestal.

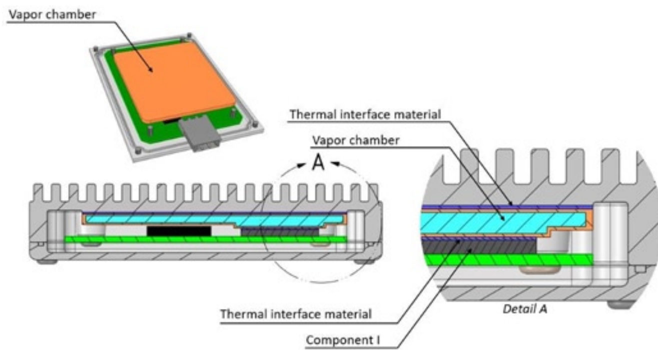

Fig. 6. Vapor chamber integrated into the housing of the analyzed device

This allowed for maximization of contact surface area between the enclosure and VC condenser region. For the sake of simulation simplification, it was assumed, that the processes of evaporation, convection, condensation and capillary transport of working fluid inside the VC can be represented as a steady state heat conduction using an isotropic material model. This approach is commonly used by simulation community. The authors of [7] and [13] presented results of separate experimental campaigns aimed at elaboration of simplified VC numerical models. In both cases, the derived VC simulation models were built from solid blocks of homogeneous material, characterized by extremely high thermal conductivity values of $8300-10000\frac{\mathrm{W}}{\mathrm{m\cdot K}}$. In [13] the authors measured the VC ability to conduct the heat in various temperatures. According to the presented results, higher operating temperature led to greater equivalent thermal conductivity of the device. This can be explained as a result of increased intensity of evaporation process and more rapid transport of the vapor inside the device cavity, which take place in elevated temperature. It can be read in [13] that the measured equivalent thermal conductivity for the device subjected to experimental testing reached ca. $9750\frac{\mathrm{W}}{\mathrm{m\cdot K}}$, when the device temperature was $50°\mathrm{C}$ above the ambient.

In the analysis described in this paper, the numerical model of VC integrated into the electronics housing was built using isotropic material, characterized by the equivalent heat conductivity equal to $k_{eq}=9000\frac{\mathrm{W}}{\mathrm{m\cdot K}}$. Figure 7 shows the simulation results obtained for the discussed model.

The simulation results show, that integration of VC into the housing of the analyzed device causes decrease in temperature of all the components, PCB and the housing. The temperature drop and uniformity is clearly visible on the top surface of the main heat source, which stayed in contact with the VC. Maximum temperature value measured on the top surface of Component I was equal to $t_{max}^{vc}=99.95°\mathrm{C}$, which can be transformed into the junction temperature of this electronic device: $t_j^{vc}=121.91°\mathrm{C}$ (using equation (4)). Hence, the main heat source junction temperature difference in the two analyzed design alternatives reached $\Delta t_j = 125.66°\mathrm{C}-121.91°\mathrm{C}=3.75°\mathrm{C}$. The obtained simulation results are combined in Tab. 2.

Figure 7 (B) depicts temperature distribution on the top side of the housing. The results show, that integration of a VC into the electronic device enclosure leads to more uniform flow of thermal energy, that is, to decreased density of heat flux, through this component.

Table 2. The results of the numerical analyses for two tested design alternatives

	Component I top surface temperature	**Component I junction temperature**
Design variant I: device housing equipped with a pedestal	103.70°C	125.66°C
Design variant II: VC integrated into the device housing	99.95°C	121.91°C

5. Expected lifetime of Component I

Silicone-based semiconductor devices operating in elevated temperature conditions undergo a number of physical and chemical degradation processes, which accelerate their failure. The most common failure mechanism that takes place in semiconductor component dies is electromigration, which consists in migration of material atoms under electric current load. The intensity of this phenomenon depends on material temperature – the higher it is, the more rapid the electromigration.

It is common to use the Arrhenius equation in order to estimate the electromigration degradation pace of semiconductor devices. However, as described in [21], if a silicone device operates in temperature above $105°\mathrm{C}$, this approach can lead to unreliable results, underestimating the failure reaction rate. The proposed in [21] procedure, which is based on empirical data, provides higher accuracy of the failure-free lifetime estimations. The procedure is based on calculation of the so-called acceleration factor AF, which is an input to equation (5) used for estimation of expected operating lifetime:

$$L_U = L_D \cdot AF \tag{5}$$

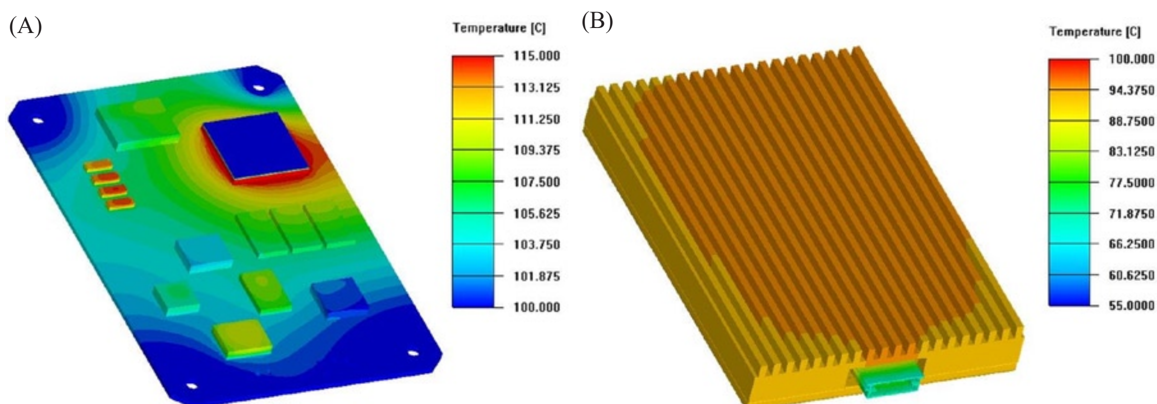

Fig. 7. Results obtained for the device equipped with a vapor chamber. Temperature field plotted for: PCB and electronic components (A) and top side of the housing (B).

where: L_D – nominal expected lifetime for junction temperature of $t_j = 105°C$, L_U – expected lifetime in specific operating temperature conditions.

According to [21], within junction temperature range of $110°C - 125°C$, the temperature dependency of the AF factor can be expressed by equation (6):

$$AF = -0.02t + 2.7 \tag{6}$$

where: $t[°C]$ denotes junction temperature in Celsius scale.

For the analyzed electronic device, the AF factor for Component I takes values of: $AF = 0.19$ and $AF^{vc} = 0.26$ for the standard cooling system and VC-based alternative, respectively. Assuming full load mission profile for this component at all times and the calculated junction temperatures of $t_j = 125.66°C$ oraz $t_j^{vc} = 121.91°C$, equation (5) leads to the conclusion, that integration of VC into the device housing will result in higher reliability of the main heat source. The change in the expected lifetime duration is equal to $0.07L_D$, therefore the device equipped with a VC is expected to operate 7% longer compared with the pedestal-based design alternative.

6. Summary

This paper presents the concept of vapor chamber integration into aluminum housing of an electronic device, operating in elevated ambient temperature of $t_{amb} = 55°C$. The effect of using VC-based cooling solution has been compared with classical, aluminum pedestal-based design. The obtained numerical simulation results demonstrate, that the use of two-phase cooling component leads to $\Delta t_j = 3.75°C$ reduction in junction temperature of the main heat source. In the assumed ambient conditions, this allows for a decrease in operating junction temperature below the limit of $t_j^{max} = 125°C$, as well as an increase in the device expected lifetime by 7%.

References

1. Aranzabal I, de Alegría I M, Delmonte N, Cova P, Kortabarria I. Comparison of the Heat Transfer Capabilities of Conventional Single-and Two-Phase Cooling Systems for an Electric Vehicle IGBT Power Module. IEEE Transactions on Power Electronics 2018; 34(5): 4185-4194, https://doi.org/10.1109/TPEL.2018.2862943.
2. Cengel Y A. Heat transfer: a practical approach, 2nd Edition. McGraw-Hill Higher Education, 2002.
3. Chainer T J, Schultz M D, Parida P R, Gaynes M A. Improving data center energy efficiency with advanced thermal management. IEEE Transactions on Components, Packaging and Manufacturing Technology 2017; 7(8): 1228-1239, https://doi.org/10.1109/TCPMT.2017.2661700.
4. Chang N, Pan S, Srinivasan K, Feng Z, Xia W, Pawlak T, Geb D. Emerging ADAS Thermal Reliability Needs and Solutions. IEEE Micro 2018; 38(1): 66-81, https://doi.org/10.1109/MM.2018.112130058.
5. Gadalla B, Schaltz E, Blaabjerg F. A survey on the reliability of power electronics in electro-mobility applications. Proceedings of: 2015 Intl Aegean Conference on Electrical Machines & Power Electronics (ACEMP), 2015 Intl Conference on Optimization of Electrical & Electronic Equipment (OPTIM) & 2015 Intl Symposium on Advanced Electromechanical Motion Systems (ELECTROMOTION) 2015; 304-310, https://doi.org/10.1109/OPTIM.2015.7427015.
6. Gu J, Pecht M. Predicting the reliability of electronic products. Proceedings of: 8th International Conference on Electronic Packaging Technology 2007; 1-8, https://doi.org/10.1109/ICEPT.2007.4441552.
7. Gurevich A, Steiner I, Huang E. Design of thermal systems based on combination of Thermoelectric and Vapor Chamber technologies. Proceedings of: 33rd Thermal Measurement, Modeling & Management Symposium (SEMI-THERM) 2017; 1-5, https://doi.org/10.1109/SEMI-THERM.2017.7896899.
8. Hager M, Gromala P, Wunderle B, Rzepka S. Affordable and Safe High Performance Vehicle Computers with Ultra-Fast On-Board Ethernet for Automated Driving. Advanced Microsystems for Automotive Applications 2018: Smart Systems for Clean, Safe and Shared Vehicles. Springer, 2019, https://doi.org/10.1007/978-3-319-99762-9_5.
9. Hammoud J, Dudley S, Apte N. Use of Heat Pipe Technology for Multi Media Thermal Management. Proceedings of: SAE 2006 World Congress & Exhibition 2006; 1-3, https://doi.org/10.4271/2006-01-0482.
10. Khazaka R, Mendizabal L, Henry D, Hanna R. Survey of high-temperature reliability of power electronics packaging components. IEEE Transactions on power Electronics 2014; 30(5): 2456-2464, https://doi.org/10.1109/TPEL.2014.2357836.
11. Ma X, Guo Y, Wang L, Ji W. Exploration of the reliability of automotive electronic power steering system using device junction electrothermal profile cycle. IEEE Access 2016; 4: 7054-7062, https://doi.org/10.1109/ACCESS.2016.2621034.
12. Mochizuki M. Latest development and application of heat pipes for electronics and automotive. Proceedings of: IEEE CPMT Symposium Japan 2017; 87-90, https://doi.org/10.1109/ICSJ.2017.8240095.
13. Niittymaki L, Biber C, Carbone M. Flexible CFD simulation model of a thin vapor chamber for mobile applications. Proceedings of: 22nd International Workshop on Thermal Investigations of ICs and Systems (THERMINIC) 2016; 152-157, https://doi.org/10.1109/THERMINIC.2016.7749044.
14. Qi F, Wang Y, Bob-Manuel C, Li H, Jones S, Li B, Chen Y, Yan Y. Advanced Cooling Solutions of High Power Automotive Module. Proceedings of: PCIM Asia 2017: International Exhibition and Conference for Power Electronics, Intelligent Motion, Renewable Energy and Energy Management 2017; 1-3.
15. Ram Sundar R, Sarweshwara Sarma N S V. Performance study of motorcycle driving-beam LED headlight with different heat sink models and LED pitch. Proceedings of: 16th IEEE Intersociety Conference on Thermal and Thermomechanical Phenomena in Electronic Systems (ITherm) 2017; 784-792.
16. Riches S, Johnston C. Electronics design, assembly and reliability for high temperature applications. Proceedings of: IEEE International Symposium on Circuits and Systems (ISCAS) 2015; 1158-1161, https://doi.org/10.1109/ISCAS.2015.7168844.
17. Robinson A J, Colenbrander J, Kempers R, Chen R. Solid and Vapor Chamber Integrated Heat Spreaders: Which to Choose and Why. IEEE Transactions on Components, Packaging and Manufacturing Technology 2018; 8(9): 1581-1592, https://doi.org/10.1109/TCPMT.2018.2822400.

18. Simon D, Boianceanu C, De Mey G, Ţopa V. Experimental reliability improvement of power devices operated under fast thermal cycling. IEEE Electron Device Letters 2015; 36(7): 696-698, https://doi.org/10.1109/LED.2015.2432128.
19. Sun L, Gu X H, Song P, Di Y. A generalized equivalent temperature model in a time-varying environment. Eksploatacja i Niezawodnosc - Maintenance and Reliability 2017; 19(3): 432-440, https://doi.org/10.17531/ein.2017.3.14.
20. Tan C M, Narula U, Kapoor D. Reliability paradox for worldwide automotive electronics. Proceedings of: IEEE Annual Reliability and Maintainability Symposium (RAMS) 2017; 1-7, https://doi.org/10.1109/RAM.2017.7889654.
21. Webber A. Calculating Useful Lifetimes of Embedded Processors: Application Report. Texas Instruments Incorporated, 2017.
22. Zeng S, Sun B, Tong C. A modified model of electronic device reliability prediction. Eksploatacja i Niezawodnosc - Maintenance and Reliability 2009; 4(44): 4-9.

Jakub KORTA

Paweł SKRUCH
AGH University of Science and Technology
Faculty of Electrical Engineering, Automatics, Computer Science and Biomedical Engineering
Department of Automatic Control and Robotics

E-mails: jakub.korta@ieee.org, pawel.skruch@agh.edu.pl